AGU ADVANCING EARTH AND SPACE SCIENCE

Earth's Future

RESEARCH ARTICLE
10.1029/2021EF001992

# Heatwaves in Southeast Asia and Their Changes in a Warmer World

**Zizhen Dong[1,2], Lin Wang[1,2], Ying Sun[3], Ting Hu[3], Atsamon Limsakul[4], Patama Singhruck[5], and Sittichai Pimonsree[6]**

[1]Center for Monsoon System Research, Institute of Atmospheric Physics, Chinese Academy of Sciences, Beijing, China, [2]College of Earth and Planetary Sciences, University of Chinese Academy of Sciences, Beijing, China, [3]National Climate Center, China Meteorological Administration, Beijing, China, [4]Environmental Research and Training Center, Pathumthani, Thailand, [5]Department of Marine Science, Faculty of Science, Chulalongkorn University, Bangkok, Thailand, [6]Atmospheric Pollution and Climate Change Research Unit, School of Energy and Environment, University of Phayao, Phayao, Thailand

**Key Points:**

- Global warming is associated with substantial increases in heatwave frequency, duration, and amplitude over Southeast Asia
- The increase of heatwave amplitude with global mean temperature is quasilinear, and that of heatwave frequency and duration are nonlinear
- A warmer future will see a higher risk ratio with rarer extreme heatwave events relative to the current climate

**Supporting Information:**

Supporting Information may be found in the online version of this article.

**Correspondence to:**

L. Wang,
wanglin@mail.iap.ac.cn

**Citation:**

Dong, Z., Wang, L., Sun, Y., Hu, T., Limsakul, A., Singhruck, P., & Pimonsree, S. (2021). Heatwaves in Southeast Asia and their changes in a warmer world. *Earth's Future*, 9, e2021EF001992. https://doi.org/10.1029/2021EF001992

Received 13 JAN 2021
Accepted 21 JUN 2021

**Author Contributions:**

**Conceptualization:** Lin Wang
**Formal analysis:** Zizhen Dong
**Funding acquisition:** Lin Wang
**Investigation:** Zizhen Dong, Lin Wang, Atsamon Limsakul, Patama Singhruck, Sittichai Pimonsree
**Methodology:** Zizhen Dong, Lin Wang, Ying Sun, Ting Hu
**Project Administration:** Lin Wang
**Resources:** Lin Wang
**Supervision:** Lin Wang
**Validation:** Zizhen Dong
**Visualization:** Zizhen Dong



**Abstract** Based on the observational dataset SA-OBS and model outputs from the Community Earth System Model Large Ensemble project, this study investigates heatwaves in Southeast Asia in the current and future warmer climate. A heatwave is detected when the daily maximum temperature exceeds the 90th percentile threshold at each grid for at least three consecutive days. Three characteristics describing the frequency, duration, and amplitude of heatwaves are examined, including the sum of heatwave days per year (HWF) satisfying the heatwave definition, the length of the longest yearly heatwave event (HWD), and the hottest amplitude of the hottest yearly heatwave event (HWA). Results indicate that increased global warming is associated with substantial changes in heatwave characteristics over Southeast Asia, with more frequent heatwaves, longer heatwave duration, and higher extreme temperatures. The increase in HWA has a linear growth against global warming levels with distinct regional differences between the Maritime Continent and the Indochina Peninsula due to their different heat content of lower atmospheric boundaries. In contrast, those in HWF and HWD have nonlinear growth characteristics. The projected warmer future tends to be associated with a higher risk ratio value with the occurrence of rarer extreme heatwaves relative to the current climate. These results reiterate the potential risks of extreme regional heatwaves if global warming is unrestricted.

**Plain Language Summary** A heatwave denotes a prolonged period that the temperature is above a prescribed threshold for several consecutive days. It usually has adverse effects on human health and the ecosystem. However, there is little knowledge of heatwaves in tropical developing countries such as those in Southeast Asia. This study investigates three characteristics, including the frequency, duration, and amplitude, of the heatwaves in the current climate and their changes in the future warmer climate in Southeast Asia based on observational datasets and outputs from a state-of-the-art model, the Community Earth System Model. Results indicate that global warming will lead to substantial changes in heatwaves over Southeast Asia. The changes are not uniform in space, especially between the Maritime Continent and the Indochina Peninsula, because the two regions have different types of land-sea distribution. Nevertheless, a consensus is that more frequent heatwaves, longer heatwave duration, and higher extreme temperature during heatwaves will occur over entire Southeast Asia in a warmer world. These changes mean that a rare heatwave, such as that occurring once-in-50-years in the current climate, will become common and happen more frequently in a warmer future.

## 1. Introduction

A heatwave is usually defined as a prolonged period that the temperature is above a prescribed threshold for several consecutive days (X.-X. Li, 2020; Seneviratne et al., 2012). Heatwaves generally have numerous adverse effects on human health (Matthews et al., 2017; Mora et al., 2017; Robine et al., 2008), ecosystem (Allen et al., 2010; Lesk et al., 2017), infrastructure (Añel et al., 2017; Auffhammer et al., 2017; X.-X. Li, 2018), agriculture (Grumm, 2011; Tebaldi & Lobell, 2018; Zampieri et al., 2017), and labor productivity (Dunne et al., 2013; Kjellstrom et al., 2009; Xia et al., 2018). For instance, the European heatwave in summer 2003 bore a close resemblance to the projection for summer in the latter part of the twenty-first

**Writing – original draft:** Zizhen Dong, Lin Wang
**Writing – review & editing:** Lin Wang

century with regional climate models (Beniston, 2004). It caused a considerable reduction of the power generation capacity in France (Añel et al., 2017) and resulted in more than 70,000 deaths in Europe (Robine et al., 2008). The heatwave in June 2019 also exerted widespread influences on countries in Central Europe (Xu et al., 2020; Xu et al., 2021). The 2013 extreme heatwave in southeast China broke the heat records of the past 141 years and caused 167 excess deaths in Pudong New Area alone, especially the females and elders (X. Sun et al., 2014). It also induced a total economic loss of 27.49 billion Chinese Yuan (~4.20 billion U.S. dollars) in Nanjing city alone due to reduced labor productivity and working capacity (Xia et al., 2018). Hence, it is essential to understand and predict how heatwaves behave to make a prior preparation or adaptation. At present, the understanding of heatwaves has improved in many regions of the world (e.g., Cowan et al., 2014; Dosio, 2017; Pfahl & Wernli, 2012; Russo et al., 2015; You et al., 2017). However, there is insufficient knowledge of how and why heatwaves behave in developing countries over tropical regions such as Southeast Asia.

Southeast Asia comprises 11 countries, with more than half a billion people (Juneng & Tangang, 2005). Its climate is modulated by the Asian-Australian monsoon system (Chang et al., 2005; Robertson et al., 2011). Heatwaves exhibited an upward trend during the past few decades (X.-X. Li, 2020; Luo & Lau, 2018; Supari et al., 2017), which are companied by the weakening of the Asian-Australian monsoon with suppressed rainfall and hot and subsiding conditions in the Indochina Peninsula (Luo & Lau, 2018). The El Niño-Southern Oscillation (ENSO) is the most critical factor influencing the precipitation and temperature over Southeast Asia (e.g., Feng et al., 2010; Hamada et al., 2002; Juneng & Tangang, 2005; McBride et al., 2003) as well as the extreme warm events (Caesar et al., 2011; Lin et al., 2018; Thirumalai et al., 2017) on the interannual timescale. Although the seasonal variation in temperature over Southeast Asia has limited fluctuation (Figure 1b), heatwaves still severely influence local people. For example, a higher intensity level of heatwaves led to more deaths from 1999 to 2008 in Northern and Central Thailand (Huang et al., 2018), and the elderly population suffered most from the spatial heterogeneity of heatwave vulnerability. Heatwave also significantly increased the risk of all cause-specific mortality in Ho Chi Minh City of Vietnam (Dang et al., 2019). In April 2016, Southeast Asia experienced a high-temperature event and broke the record that traces back to the mid-twentieth century (Thirumalai et al., 2017). In Thailand, the duration of scorching weather in 2016 set a new record after 1950, and the maximum temperature in each day of April all exceeded 40°C with one day reaching 44.3°C (Associated Press, 2016; Thai Meteorological Department, 2017). Such an event disrupted crop production and resulted in societal distress and colossal energy consumption (Thirumalai et al., 2017).

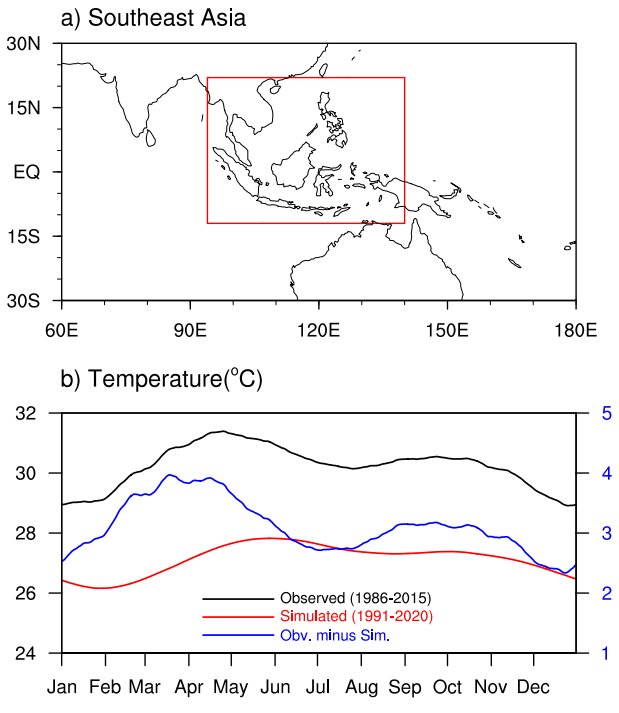


**Figure 1.** (a) Domain of Southeast Asia defined in this study (12°S–22°N and 94°E–140°E, indicated by the red rectangle). (b) The observed (black line) and simulated (red line) climatology of the annual cycle of $T_{max}$ (unit: °C) averaged over Southeast Asia and their difference (blue line). The observed and simulated climatologies of annual cycles are based on the 30 years 1986–2015 and 1991–2020, respectively.

It is a consensus that the frequency and intensity of extreme events will increase in the future with global warming (Meehl & Tebaldi, 2004; Perkins-Kirkpatrick & Gibson, 2017; Seneviratne et al., 2012). The Intergovernmental Panel on Climate Change (IPCC) Fifth Assessment Report (AR5) suggests that the near-term increases in the seasonal and annual mean temperature are more prominent in the tropics and subtropics than in mid-latitudes relative to the natural variability (Stocker et al., 2013). It implies that Southeast Asia may suffer more from global warming than other regions of Asia. Hence, it is essential to understand heatwaves over Southeast Asia in-depth regarding their possible changes in a warmer world because of the vital influences of heatwaves on regional ecosystems and society. In this regard, Dosio et al. (2018) compared the global occurrence of heatwave events between two warming levels. They showed that in a 1.5°C warmer world, a significant increase in intensity and frequency of heatwave events would occur over Africa, central and south America, and Southeast Asia (their Figure 1c), and that in a 2°C warmer world, the increase of magnitude will double over most of the globe. They also suggested that approximately 57.6% of land in Southeast Asia will face extreme heatwaves at least once every 20 years. Zhu et al. (2020) projected

that potentially conspicuous temperature extremes primarily concentrate on the densely populated coastal regions of the main islands.

Despite the extensive research outlined above, there remain some gaps and deficiencies in understanding heatwaves over Southeast Asia. On the one hand, many studies focus how heatwaves will change at the end of the 21st century (e.g., Coffel et al., 2017; Mora et al., 2017), but a tendency in the scientific community and concern of the public is the changes of heatwaves at different global warming levels after the Paris Agreement. On the other hand, two specific global warming levels, that is, 1.5 and 2°C above the pre-industrial period, have been widely considered in the heatwave studies (e.g., Dosio et al., 2018; Russo et al., 2017; Zhu et al., 2020). Nevertheless, it is necessary to include more warming levels to understand how regional heatwaves respond to global or regional warming. Such understanding is crucial because of its scientific importance and usefulness for countries in this region to make decisions on their development routes. Therefore, it is necessary and essential to investigate possible changes of heatwaves over Southeast Asia in a warmer world by considering sufficient heatwave characteristics and more warming levels. This study uses three heatwave characteristics defined by the percentile-based threshold to examine the behaviors of heatwaves over Southeast Asia and their projections in a warmer world. Section 2 introduces the data sets and methodologies. Section 3 delineates the warming results and their changes in the future. Finally, section 4 provides the conclusion and discussion.

## 2. Data and Method

### 2.1. Observational and Model Data

A daily land-only observational gridded data set for Southeast Asia named SA-OBS (van den Besselaar et al., 2017) is used in this study. SA-OBS is based on the station data provided by meteorological services of Southeast Asian countries within the Southeast Asian Climate Assessment and Dataset project (SACA&D). This data set covers the area (20°S–25°N, 80°E–180°E) and includes precipitation, minimum, mean, and maximum temperature on a 0.25° × 0.25° latitude-longitude grid from 1981 to 2017. The global historical gridded data set of surface temperature, version 4.2.0 (HadCRUT4, Morice et al., 2012), is used to represent the observed global warming. Southeast Asia is defined as the area extending from 12°S to 22°N and from 94°E to 140°E (rectangle in Figure 1a), consistent with Juneng and Tangang (2005).

The model data on the 0.9° × 1.25° latitude-longitude grid are from daily outputs of a large ensemble simulation conducted with the Community Earth System Model (CESM) version 1 under the Coupled Model Intercomparison Project (CMIP) Phase five (CMIP5) configuration. This CESM large ensemble (CESM-LE) simulation contains 40 independent runs covering the period 1920–2100 under historical forcing (1920–2005) and RCP8.5 forcing (2006–2100) with slight differences in the initial atmospheric conditions (Kay et al., 2015). The simulated maximum and mean daily temperatures are used to project future heatwaves, and the period 1850–1900 is used to estimate the pre-industrial era. In order to better compare the observational results with simulations, the SA-OBS data set is converted to the model resolution by averaging all available 0.25° × 0.25° data within the 0.9° × 1.25° model grid.

### 2.2. Heatwave Definition and Characteristics

There are usually two approaches to define a prescribed threshold for heatwaves (Robinson, 2001). One centers on the general thermoregulation of the human body and is referred to as the fixed absolute threshold. The other centers on local adaptations to climate and is based on the percentile (relative) threshold. There is no consensus on which approach is better because they emphasize different purposes of the application. This study employs the latter approach because the former approach misrepresents heatwaves in the mainland of Southeast Asia (i.e., Indochina Peninsula) and the Maritime Continent because of the different heat contents of atmospheric lower boundaries. For example, the heatwave definitions based on different fixed thresholds (i.e., 35, 36, and 37°C) significantly inhibit the observed heatwaves over Indonesia (Figure S1). In this study, the 90th percentile of the daily maximum temperature ($T_{max}$) is the threshold at each grid for each calendar day (e.g., Cowan et al., 2014; Perkins & Alexander, 2013; Perkins et al., 2012; Perkins-Kirkpatrick & Lewis, 2020), accounting for the seasonal cycle (Fischer & Schär, 2010). This percentile

is based on a centered 15-days window over 1981–2010 in SA-OBS to produce a reasonable sample size. Then a heatwave is detected when at least three consecutive days are above the threshold.

This study considers three heatwave characteristics, including frequency, duration, and amplitude, which are also used in Perkins and Alexander (2013). Heatwave frequency (HWF) is defined as the sum of participating heatwave days per year that satisfy the heatwave criterion. Heatwave duration (HWD) is defined as the longest yearly heatwave event's length (in days). Heatwave amplitude (HWA) is defined as the hottest day (amplitude) of the hottest yearly heatwave event. As such, HWD and HWA measure a single heatwave event each year, and HWF measures all yearly heatwaves. Humidity is another variable often involved in heatwaves because high humidity may aggravate the impacts of heatwaves on human thermoregulation (Kravchenko et al., 2013; Schär, 2016). Quantities combining temperature and humidity are often used to define moist heatwaves (D. Li et al., 2020; X.-X. Li, 2020; Mora et al., 2017; Schoof et al., 2017), such as the wet-bulb temperature (Coffel et al., 2017; Raymond et al., 2020) and the apparent temperature (Matthews et al., 2017; Russo et al., 2017). Nevertheless, this study only considers dry heatwaves because of the limited availability of daily humidity data in both the observation and model outputs. Trends of various heatwave characteristics are derived from the nonparametric Theil-Sen slope estimate (Sen, 1968), and the statistical significance of trends is based on the Mann-Kendall test (Mann, 1945).

### 2.3. Bias Correction for Model Data

The model simulated temperatures usually have some regional biases (e.g., in CMIP5 models). Their median biases of the seasonal and annual mean temperature range from about −3 to 1.5°C in 26 global land areas relative to the observation during 1986–2005 based on temperature data from the CRU TS3.10 data set (Flato et al., 2013). As a result, the heatwave characteristics in simulations may hamper the correct calculation because of the model bias. In order to examine the bias in CESM, Figure 1b shows the observed and simulated annual cycles of $T_{max}$ averaged over Southeast Asia. It reveals that the observed annual cycle is weak, with the highest $T_{max}$ between April and May. The CESM model has a cold bias and a delayed peak in the annual cycle compared to the observation.

In order to reduce the possible influence of the cold bias in CESM on heatwave projection, a bias correction procedure is applied to the model data by replacing the modeled seasonal cycle of $T_{max}$ over Southeast Asia with the observed one. This procedure follows Y. Sun et al. (2018) and includes three steps. First, the seasonal cycle of the observed $T_{max}$ is computed over the 30 years 1986–2015 with a running-average window of 15 days. Second, similar calculations are applied to each run of the CESM simulations using another 30 years 1991–2020. Third, the seasonal cycles from individual model runs are replaced by the observed seasonal cycle in step one to produce the bias-corrected model data for 1920–2100. In this way, the bias-corrected procedure only adjusts the cold bias of $T_{max}$ in CESM but does not adjust the variability (Y. Sun et al., 2018). When we compare the heatwave projections based on the modeled data with (Figure 4) and without (Figure S2) bias-correction, it is evident that the future changes of heatwaves over Southeast Asia perform better after bias-correction, especially regarding the available grids that experience heatwaves in the current climate. Thus, the subsequent analyses are all based on the bias-corrected model data.

Note that the period 1991–2020 is used in CESM for the bias correction because the modeled global mean surface temperature (GMST) during this 30-years climatology has increased the same amount as the observed GMST during the observational 1986–2015 relative to the pre-industrial era. The observed 30-years value of GMST for the period 1986–2015 is 0.686°C (Y. Sun et al., 2018) above the pre-industrial era (1850–1900) average based on HadCRUT4, while the modeled GMST for 1986–2015 is 0.578°C above its pre-industrial value. It means that the CESM simulations underestimate the observed global warming. The 30-year period for the modeled GMST, which is the closest to the observed warming level during 1986–2015, is 1991–2020, and the warming level is 0.693°C. Therefore, we consider the 30-year period 1991–2020 in simulations equivalent to the observed 30-year period 1986–2015 and use this period for bias correction in the CESM model.

### 2.4. Global Warming Levels

The global warming level indicates the increase of GMST related to the pre-industrial baseline period, which is defined as 1850–1900 and widely used in the international climate policy, such as the Paris Agreement. For example, the current climate is approximately at the 1°C warming level because the observed GMST of 2016 is 1.1°C above the pre-industrial level (Y. Sun et al., 2018; World Meteorological Organization, 2017). In this study, several different global warming levels are considered, including the current climate 1.0°C warming level and several future warming levels, such as the 1.5, 2.0, 3.0, 4.0, and 4.5°C levels. The above global warming levels are defined based on the 10-year period during which the GMSTs are above the pre-industrial baseline (1850–1900) in CESM simulations under the RCP8.5 scenario. As such, the periods to define the 1.0, 1.5, 2.0, 3.0, 4.0, and 4.5°C warming levels are 2011–2020 (0.973°C), 2025–2034 (1.490°C), 2036–2045 (1.952°C), 2056–2065 (2.973°C), 2075–2084 (3.990°C), and 2086–2095 (4.495°C), respectively, where the values in brackets indicate the averaged GMST during the 10-year periods.

### 2.5. Risk Ratio

The risk ratio (RR), also known as the relative risk, is used to measure the changes in the probability of extreme heatwaves in the future. It is defined as RR = *P1/P0*, where *P1* is the event probability in the future climate (refers to the different warming levels), and *P0* is the event probability in the current climate (2011–2020 in the simulations). The RR is a concept to describe the change in probability of a low probability event that is used in the event attribution (National Academies of Sciences, Engineering, & Medicine, 2016). In this study, the RR of three types of extreme (i.e., low probability) heatwave events is considered, including that occurs once in 5, 10, and 50 years in the current climate. Thus, *P0* is fixed to 0.2, 0.1, and 0.02. For example, if RR equals 2.5 for the 5-years event, *P1* equals 0.5. It means the once-in-5-years event in the current climate will become a once-in-2-years event in the future.

The empirical formula $P = (m\text{-}0.31)/(N\text{+}0.38)$ (Jenkinson, 1977) is used to estimate the probabilities of *P1*. The sample size *N* equals 400 because each of the 40 runs has 10 years for each warming level. *P* is the probability that the random value is less than or equal to the value ranked *m* in ascending order based on the 400 years data from 40 simulations at different warming levels. The uncertainty in RR with a 5%–95% range for the future warming level is determined using a bootstrap procedure in two steps (Y. Sun et al., 2018). First, we estimate the return levels of the number of HWF and HWD and the amplitude of HWA for 5-, 10-, and 50-years return periods in the current climate (2011–2020) by drawing random 400 years data from the 40 CESM runs with replacement. This procedure is repeated 500 times to obtain 500 sets of return levels for the current climate. Second, we extract 40 10-years samples from the 40 runs at a warmer level and calculate a set of *P1* corresponding to each of the 500 sets of the return levels in the current climate. This procedure produces 500 sets of RR values. The above process is repeated 500 times to result in 500 × 500 sets of RR, from which the 5%–95% uncertainty range for the future is determined.

## 3. Results

### 3.1. Southeast Asian Heatwaves in Observation and CESM

Area-averaged HWF, HWD, and HWA anomalies across Southeast Asia relative to 1981–2010 in observations (relative to 2011–2020 in simulations) are calculated by averaging all available grids where heatwaves occur. The use of available grids is because heatwaves may not occur at every grid, considering the restriction of three consecutive days exceeding the threshold temperature in the heatwave definition. The chosen grids for averaging must have at least five heatwaves during the recent 10-years 2008–2017 in observation or 200 heatwaves during the current climate 2011–2020 in 40 runs. Figures 2a–2b show that HWF and HWD have a clear and nearly linear relationship with the area-averaged annual mean temperature over Southeast Asia in observation and that HWA has a more nonlinear relationship. A similar relationship is observed with the three heatwave characteristics when the temperature over Southeast Asia is replaced with the GMST (Figures 2c–2d). This result indicates that with the higher GMST and Southeast Asian annual mean temperature, Southeast Asia undergoes more frequent heatwaves, longer heatwave duration, and higher extreme temperature in the past three decades. The correlation coefficients between GMST (annual mean temperature of Southeast Asia) and the observed HWF, HWD, and HWA are 0.74 (0.88), 0.73 (0.87), 0.45

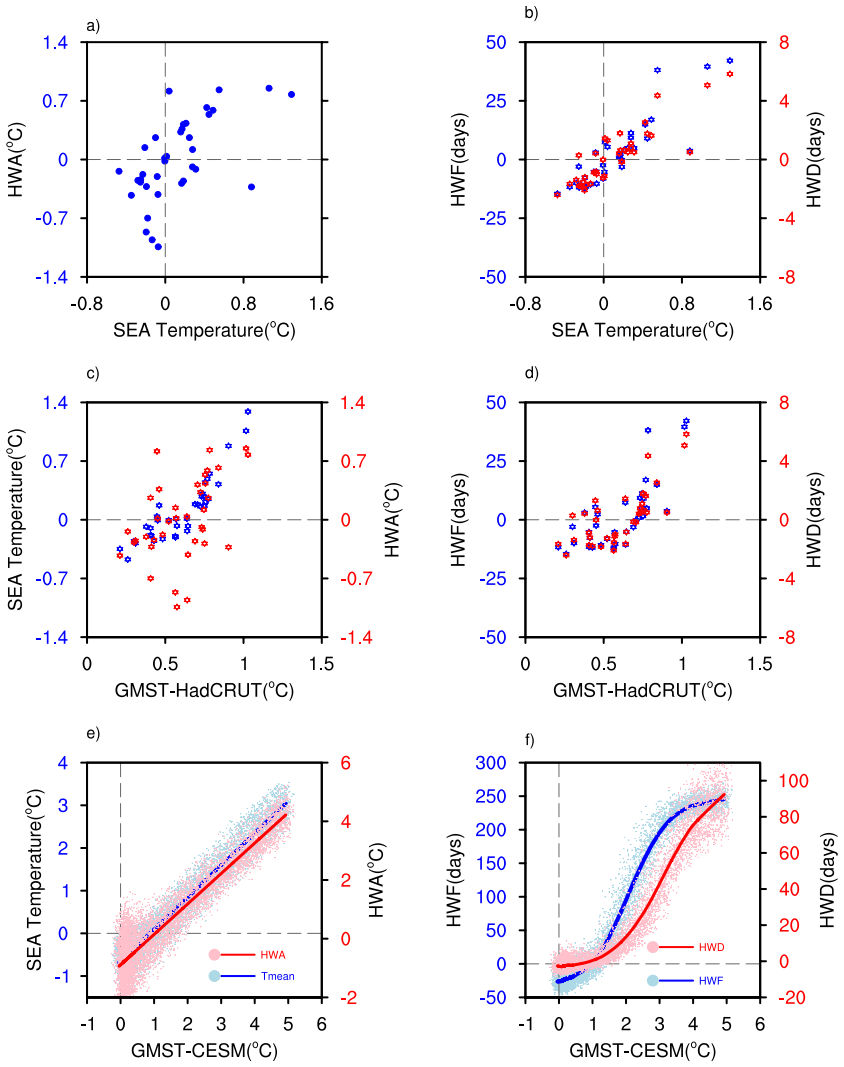


**Figure 2.** (a) Scatter plot of hottest amplitude of the hottest yearly heatwave event (HWA) anomalies (unit: °C) versus annual mean Southeast Asian temperature ($T_{SEA}$) anomalies (unit: °C) in observation. (b) is the same as (a), but for heatwave days per year (HWF) anomalies (blue dots, left axis, unit: days) and length of the longest yearly heatwave event (HWD) anomalies (red dots, right axis, unit: days) in observation. (c) Scatter plot of annual mean $T_{SEA}$ anomalies (blue dots, left axis, unit: °C) and HWA anomalies (red dots, right axis, unit: °C) versus global mean surface temperature (GMST) anomalies (unit: °C) in observation. (d) is the same as (c), but for HWF anomalies (blue dots, left axis, unit: days) and HWD anomalies (red dots, right axis, unit: days) in observations. (e)–(f) are the same as (c)–(d), but based on the Community Earth System Model-large ensemble (CESM-LE) outputs. In (a)–(d), the HWA, HWF, and HWD are averaged over grids with at least five heatwaves during the recent 10-years 2008−2017 in observation, and the anomalies are defined relative to 1981–2010 mean. In (e)–(f), the HWA, HWF, and HWD are averaged over grids with at least 200 heatwaves in the 40 runs during the 10-years current climate (2011–2020) in CESM-LE. Anomalies of $T_{SEA}$ and heatwave characteristics are defined relative to the current climate (2011–2020) in simulations, and anomalies of GMST are defined relative to the pre-industrial level (1850–1900). Dots represent values from individual runs, and solid lines are smoothing lines using the weighted least squares fit.

(0.60), respectively, indicating that the changes in the heatwave frequency, duration, and amplitude all track well with the changes in the observed GMST and the Southeast Asian annual temperature. Moreover, changes in the heatwave frequency and duration track better than changes in the heatwave amplitude do. It implies that global warming is the primary driver for the more frequent and prolonged heatwaves in Southeast Asia. However, factors other than global warming may be critical to determine the strength of heatwaves in Southeast Asia. A 1°C increase in GMST warming level corresponds to a 1.1°C increase in HWA, 51.6, and 7.0 days increase in HWF and HWD in observation, respectively. The CESM-LE captures these

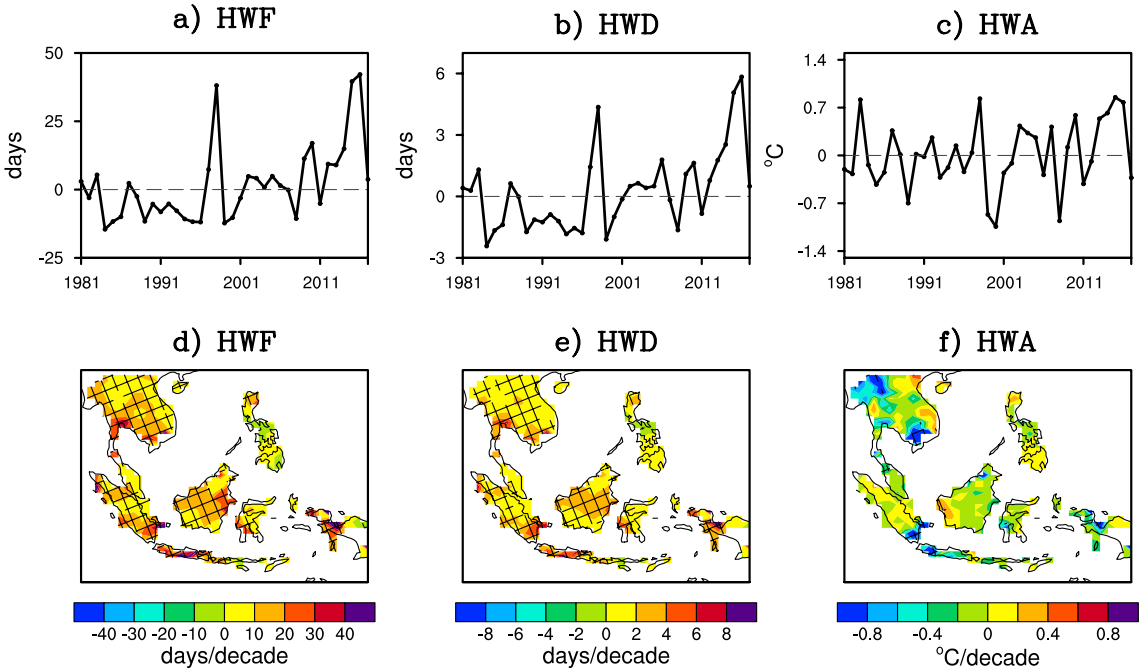


**Figure 3.** The time series of area-averaged (a) heatwave days per year (HWF) (unit: days), (b) length of the longest yearly heatwave event (HWD) (unit: days), and (c) hottest amplitude of the hottest yearly heatwave event (HWA) (unit: °C) anomalies (relative to 1981–2010 mean) over Southeast Asia calculated by SA-OBS during 1981–2017. The trends of (d) HWF (unit: days/decade), (e) HWD (unit: days/decade), and (f) HWA (unit: °C/decade) in Southeast Asia as detected by SA-OBS using the nonparametric Theil-Sen slop estimate. The hatches represent trends exceeding the 95% confidence level using the Mann-Kendall test. The time series in (a)–(c) are averaged only over the colored regions in (d)–(f).

observed heatwave characteristics well when the modeled GMST increase is below 1°C (Figures 2e–2f). HWA and Southeast Asia's annual mean temperature in a warmer world have a more linear relationship with GMST, whereas HWF and HWD show a nonlinear relationship with GMST. When GMST increases by 3.0°C, the growth rate of HWF slows down (Figure 2f) because heatwave days in a year gradually saturate (Figure 5a).

In order to further depict the observed changes in heatwave behaviors, Figure 3 shows the area-averaged time series and the long-term trends of heatwave characteristics over Southeast Asia. The area-averaged heatwave over Southeast Asia shows an apparent upward trend in the time series of HWF and HWD (Figures 3a–3b) and a weak trend in HWA (Figure 3c), consistent with Figure 2. Their peaks coincide with strong El Niño years, such as 1998, 2010, and 2016. The correlation coefficients between the Niño 3.4 index of the preceding winter and HWF, HWD, and HWA are 0.56, 0.54, and 0.82, respectively, all exceeding the 99% confidence level based on the two-tailed Student's *t*-test. This result indicates substantial impacts of El Niño on temperature extremes over Southeast Asia, consistent with interpretations of the previous paragraph and results of previous studies (e.g., X.-X. Li, 2020; Lin et al., 2018; Thirumalai et al., 2017).

The significantly upward trends are mainly located over northern Philippines, Indochina Peninsula, southwestern Kalimantan, Sumatra, Java, Sulawesi, and western New Guinea for HWF and HWD (Figures 3d–3e). In contrast, no significant trends are observed over most regions in Southeast Asia for HWA (Figure 3f). The consistent spatial and temporal variations of HWF and HWD are because the total heatwave days directly influence heatwave length and occurrence frequency. A change in total days participating in heatwaves means the duration (HWD) and their yearly number (HWF) must also change accordingly (Perkins & Alexander, 2013). In contrast, HWA reflects the amplitude of the hottest yearly event and is little affected by an increase in HWF or HWD. April is the hottest month over Southeast Asia on average (Figure 1b); thus, the hottest day of the hottest heatwave event (i.e., HWA) usually occurs in this month. The temperature variation in April primarily depends on the internal variability such as El Niño other than long-term warming (Thirumalai et al., 2017). It partly explains the insignificant long-term trends of HWA in observation (Figure 3f).

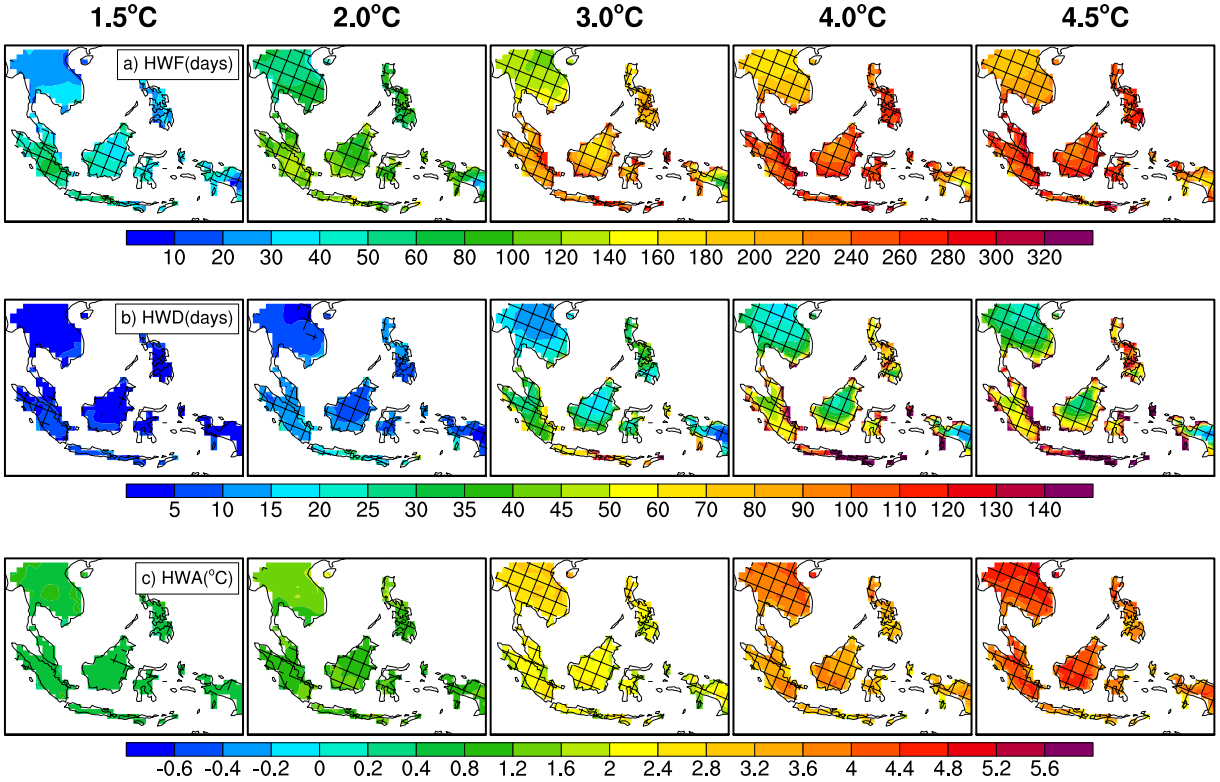


**Figure 4.** Projected changes in (a) heatwave days per year (unit: days), (b) length of the longest yearly heatwave event (unit: days), and (c) hottest amplitude of the hottest yearly heatwave event (unit: °C) under 1.5, 2.0, 3.0, 4.0, and 4.5°C global warming levels relative to the current climate as simulated by the Community Earth System Model-large ensemble. Hatches represent the changes exceeding the 95% confidence level based on the two-tailed Student's *t*-test.

### 3.2. Projected Changes of Heatwave in a Warmer World

Figure 4 shows the projected changes in heatwaves at different warming levels and suggests that higher global warming levels will make heatwaves worse and bring significant adversity to people's lives. In a warmer future, heatwaves tend to occur most of the time in a year. For example, under the 2.0°C global warming, approximately 50 heatwave days are observed over Indochina, with the most prolonged duration below 10 days (Figures 4a–4b). However, when GMST rises by 4.5°C, there are as many as 180 and 280 heatwave days over Indochina and Maritime Continent, respectively, and the duration increases accordingly. It means that

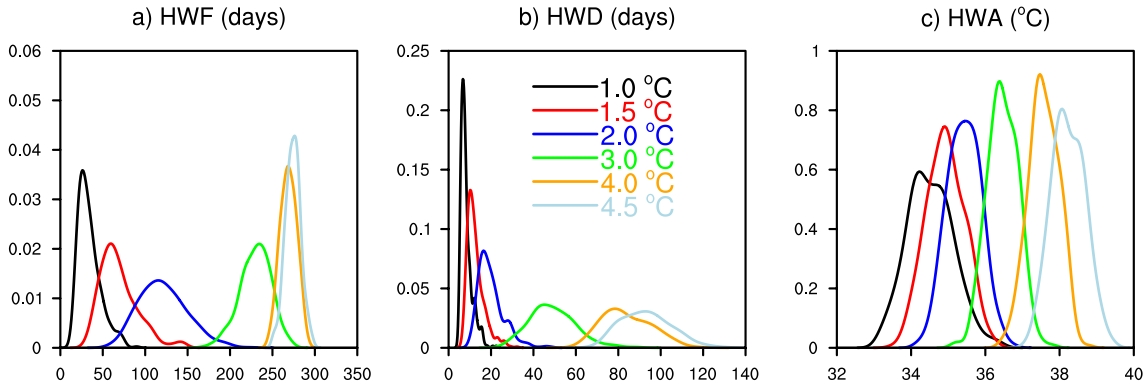


**Figure 5.** Projected changes in the kernel-smoothed probability density estimate of (a) heatwave days per year (unit: days), (b) length of the longest yearly heatwave event (unit: days), and (c) hottest amplitude of the hottest yearly heatwave event (unit: °C) under 1.0°C (black lines), 1.5°C (red lines), 2.0°C (blue lines), 3.0°C (green lines), 4.0°C (orange lines), and 4.5°C (light-blue lines) global warming levels based on the CESM-LE outputs. Values are calculated and averaged over the grids with at least one heatwave per two years in the current climate.

**Table 1**
*Projected Changes in Estimated Probability Distributions (5%, Median, and 95% Values, Respectively, Left to Right, Separated by Slashes) of Heatwaves Characteristics (i.e., HWF in Days, HWD in Days, and HWA in °C) Under Different Global Warming Levels, Corresponding to Figure 5*

| Global warming level | HWF (days) | HWD (days) | HWA (°C) |
|---|---|---|---|
| 1.0°C | 6.0/51.5/96.1 | 3.7/13.6/23.2 | 32.7/34.8/36.8 |
| 1.5°C | 18.2/88.4/157.0 | 5.1/19.5/33.7 | 33.1/34.9/36.6 |
| 2.0°C | 41.2/141.7/240.0 | 7.2/29.4/51.1 | 33.8/35.5/37.1 |
| 3.0°C | 155.5/220.8/284.6 | 18.0/57.0/95.0 | 34.9/36.5/38.1 |
| 4.0°C | 236.8/268.6/299.7 | 49.7/89.2/127.8 | 36.1/37.6/39.0 |
| 4.5°C | 244.0/274.0/303.3 | 58.8/98.9/138.2 | 36.7/38.3/39.7 |

Abbreviations: HWA, hottest amplitude of the hottest yearly heatwave event; HWD, length of the longest yearly heatwave event; HWF, sum of heatwave days per year.

what used to be an unusual phenomenon (i.e., heatwave) can become a common event in a warmer world. The projected significant increase of HWF is first observed over Indonesia, Malaysia, and parts of the Philippines when the GMST warming level is below 2.0°C, and it can further spread to Indochina Peninsula when the GMST warming level reaches and exceeds 2.0°C (Figure 4a). Similar responses of HWD and HWA to the GMST warming are also observed regarding the spatial evolution, and the critical temperature of the GMST warming is 3.0°C (Figures 4b–4c). These results indicate that Indochina Peninsula has a delayed response to the increased GMST compared with the rest regions of Southeast Asia. On the other hand, the increase of HWF and HWD shows significant regional differences and is faster over the Maritime Continent than over the Indochina Peninsula at the same warming level (Figures 4a–4b). In contrast, the increase of HWA shows a different pattern to HWF and HWD, with a faster increase over the Indochina Peninsula (Figure 4c).

The different responses of heatwave days (i.e., HWF and HWD) and extreme temperature (i.e., HWA) to the increased GMST are rooted in the different lower atmospheric boundaries and climate between the Maritime Continent and Indochina Peninsula. The Maritime Continent consists of many islands in the western Pacific Ocean. The large heat content of the surrounding ocean leads to a slower temperature increase over the Maritime Continent than over the Indochina Peninsula. As a result, higher extreme temperature (i.e., HWA) is projected over the Indochina Peninsula when the GMST increases. Meanwhile, the criteria temperature to define heatwaves in the current climate is lower over the Maritime Continent than over the Indochina Peninsula. Hence, there is more space for the heatwave-free grids over the Maritime Continent to meet the criteria of a heatwave when the GMST rises. The responses of heatwaves to global warming show distinct regional differences due to the different heat content of lower atmospheric boundaries. The different responses imply that using a relative threshold to define climate extremes over Southeast Asia better reflects the regional characteristics of Southeast Asian climate than using a fixed threshold.

### 3.3. Projected Changes in Probability Distributions of Heatwaves

Figure 5 shows the estimated probability distributions of heatwave characteristics under different warming levels. These heatwave characteristics are averaged over the grids, where the number of experienced heatwaves in the current climate is at least 200 in the 40 simulations. The distributions of heatwave characteristics show a consistently increasing trend with the increased GMST. For example, changes in the probability distribution of HWF (Figure 5a) shifts rightward with wider extension, indicating an increase in both its mean and variability before GMST increases by 4.0°C. They become narrower and shift to the right at a slower pace when the increase of GMST exceeds 4.0°C. The estimated median values (the corresponding 5%–95% range) of HWF are 51.5 days (6.0–96.1 days), 88.4 days (18.2–157.0 days), 141.7 days (41.2–240.0 days), 220.8 days (155.5–284.6 days), 268.6 days (236.8–299.7 days), 274.0 days (244.0–303.3 days) for the 1.0, 1.5, 2.0, 3.0, 4.0 , and 4.5°C global warming levels (Table 1), respectively. This result implies a gradual saturation of days participating yearly heatwaves over Southeast Asia, consistent with Figure 2f. It also means that heatwaves can occur on nearly any day of a year when the increase of GMST exceeds 4.0°C.

Changes in the probability distribution of HWD and HWA also show similar rightward shifts (Figures 5b–5c) to the HWF. The width of the probability distribution of HWD keeps widening as the GMST increases, indicating larger variability of the HWD in a warmer world. The median values (the corresponding 5%–95% range) of HWD are 13.6 days (3.7–23.2 days), 19.5 days (5.1–33.7 days), 29.4 days (7.2–51.1 days), 57.0 days (18.0–95.0 days), 89.2 days (49.7–127.8 days), 98.9 days (58.8–138.2 days) for the 1.0, 1.5, 2.0, 3.0, 4.0, and 4.5°C GMST levels (Table 1). In contrast, the width of the probability distribution of HWA becomes slightly narrower, suggesting small changes and slight decreases in the variability of HWA in the warmer future. The estimated median values and corresponding 5%–95% range of HWA are 34.8°C (32.7–36.8°C), 34.9 °C (33.1–36.6°C), 35.5°C (33.8–37.1°C), 36.5°C (34.9–38.1°C), 37.6°C (36.1–39.0°C), and 38.3°C (36.7–39.7°C) for the

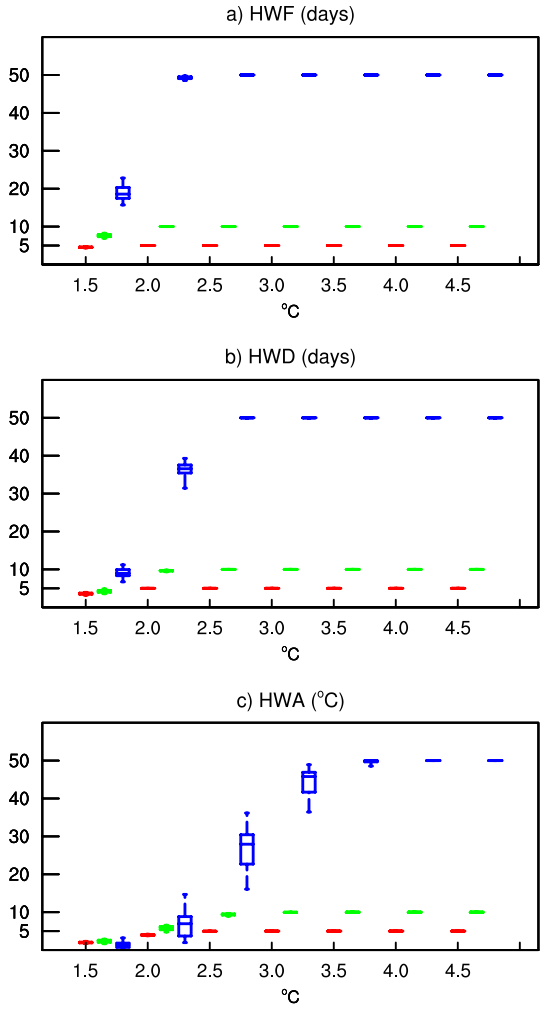


**Figure 6.** Box plots with the 5%–95% uncertainty range of risk ratio (*Y*-axis) for (a) heatwave days per year (unit: days), (b) length of the longest yearly heatwave event (unit: days), (c) hottest amplitude of the hottest yearly heatwave event (unit: °C) of extreme heatwave events with the return periods of 5-years (red), 10-years (green), and 50-years (blue) in the current climate (2011–2020) under different global warming levels (*X*-axis) as simulated by Community Earth System Model-large ensemble. Values are calculated over the grids with at least one heatwave per two years in the current climate.

current climate and under different global warming levels (Table 1). The median value of HWA increases almost linearly against GMST, consistent with Figure 2e. In short, Figure 5 provides more intuitive insights on the changes of heatwaves over Southeast Asia in a warmer world, where more frequent heatwaves, longer heatwave duration, and higher extreme temperature during heatwaves will occur.

### 3.4. Projected Changes in Risk Ratio of Heatwaves

When the GMST rises to a certain level, rare extreme heatwaves in the current climate, such as that observed in 2016 (Thirumalai et al., 2017), may become common. In order to measure this possibility, the projected RR for different heatwave characteristics is examined. Figure 6 displays the RR under different global warming levels for three extreme heatwave events with 5-, 10-, and 50-years return periods in the current climate. Significant increases in RR are projected under a warmer world relative to the current climate. For instance, the RR for the current 5-years HWA event under 2.5°C level is 5 (Figure 6c). It means that the 5-years HWA extreme event will have a probability of one and occur every year. The RR of HWA for a 50-years event under the 2.0°C global warming level is seven, which means that the rare once-in-50-years heatwave event will occur every seven years (Figure 6c). The RR of HWA will saturate at 50 when the increase of GMST reaches 4.0°C. It means that the extreme once-in-50-years event with the probability of 0.02 in the current climate will have a probability of 1 under 4.0°C warming level and that one of the worst events in the current will become a common event in the future. Similar conclusions can be reached for HWF and HWD (Figures 6a–6b). Moreover, for the same type of events (e.g., once-in-5-years event), the GMST that RR needs to saturate (i.e., RR = 1) is lower for HWF and HWD than for HWA. In other words, RR for HWF and HWD is larger than that for HWA at the same warming level. It means that the risk of experiencing more frequent extreme heatwaves is higher than that of experiencing stronger heatwaves for a particular warming level. For example, RR of HWF and HWD saturates at 2.0°C (2.5°C) warming level for a 5-years (50-years) event, and RR of HWA equals 1 at 2.5°C (4.0 °C) warming level.

## 4. Conclusion and Discussion

Based on the observational data SA-OBS and the model outputs from the CESM-LE, this study investigates the heatwave characteristics over Southeast Asia in the current and future warmer climate. A heatwave is detected when the daily $T_{max}$ is above the 90th percentile threshold for each calendar day at grid level for at least three consecutive days. Three heatwave characteristics are examined, including the heatwave frequency (HWF), heatwave duration (HWD), and heatwave amplitude (HWA). All these heatwave characteristics over Southeast Asia track well with the increased GMST in the past decades and a warmer world (Figure 2). The long-term trends of HWF and HWD show a significant upward trend over most areas of Southeast Asia, while no significant trend in HWA is observed (Figure 3). The projected changes in heatwave characteristics are examined under different global warming levels, including 1.0, 1.5, 2.0, 3.0, 4.0, and 4.5°C. Results indicate that the increased global warming level is associated with more frequent heatwaves, longer heatwave duration, and higher extreme temperature (Figure 4), consistent with the rightward shift of probability distributions against GMST (Figure 5). Three types of extreme heatwave events with 5-, 10- and 50-years return periods are also examined by the risk ratio (RR) values at different warming levels (Figure 6). A warmer future is projected to be associated with a higher RR value with rarer extreme heatwaves.

The finding of this study is overall consistent with previous studies (e.g., Coffel et al., 2017; Dosio et al., 2018; Mora et al., 2017; Russo et al., 2017; Zhu et al., 2020), and it provides additional information in several aspects via considering more global warming levels. For example, it indicates that the global warming level primarily drives changes in the frequency and duration of heatwaves over Southeast Asia. In contrast, both global warming and ENSO control changes in the strength of heatwaves. As a whole, the projected increase of HWA against GMST is quasilinear, but those of HWF and HWD are nonlinear (Figure 2). Besides, it shows how different heatwave characteristics evolve with different global warming levels and their regional features, with late heatwave response to the increased GMST over the Indochina Peninsula than over the Maritime Continent. These findings may enrich our knowledge and capability to understand and adapt to future changes of heatwaves over Southeast Asia.

The current study is based on the relative threshold (i.e., 90% percentile) to define heatwaves, but a parallel analysis was also performed based on the fixed threshold. Results indicate that the relative threshold can better capture the regional characteristics of heatwaves in the presence of complicated land-sea distribution and topographies in Southeast Asia (not shown). Hence, a percentile-based approach is recommended to define climate extremes, such as heatwaves in Southeast Asia. Meanwhile, this study investigates dry heatwaves, but it is also necessary and essential to consider moist heatwaves because humidity can also modulate the thermal stress of dwellers (e.g., D. Li et al., 2020; X.-X. Li, 2020; Mora et al., 2017; Schoof et al., 2017), especially over the Maritime Continent. The role of humidity needs to be taken into account in future studies on Southeast Asian heatwaves. Last but not least, this study is based on the CESM-LE simulations and may have some model dependency. Using more models such as those participating in CMIP Phase 6 (CMIP6) and more emission scenarios would be helpful and may overcome some disadvantages of using one model (e.g., Seneviratne et al., 2016). It is difficult for us to perform such analyses at the moment due to our limited resources. The analysis with CMIP6 data is planned for the near future.

## Data Availability Statement

The SA-OBS data are available from https://sacad.database.bmkg.go.id/dailydata/index.php. The HadCRUT4 data are available via https://www.metoffice.gov.uk/hadobs/hadcrut4/. The CESM-LE data are available from http://www.cesm.ucar.edu/projects/community-projects/LENS/data-sets.html.

**Acknowledgments**
We thank the four anonymous reviewers and the editor Dr. Prof. Kelly Caylor for their valuable comments and suggestions to improve the manuscript during the four rounds of reviews. The work was supported by the National Natural Science Foundation of China (41925020, 41721004, 41661144016).

## References

Allen, C. D., Macalady, A. K., Chenchouni, H., Bachelet, D., McDowell, N., Vennetier, M., et al. (2010). A global overview of drought and heat-induced tree mortality reveals emerging climate change risks for forests. *Forest Ecology and Management*, *259*(4), 660–684. https://doi.org/10.1016/j.foreco.2009.09.001

Añel, J. A., Fernández-González, M., Labandeira, X., López-Otero, X., & De la Torre, L. (2017). Impact of cold waves and heat waves on the energy production sector. *Atmosphere*, *8*(11), 209. https://doi.org/10.3390/atmos8110209

Associated Press. (2016). *Scorching heat wave in Thailand is longest in 65 years*. Retrieved from http://www.chicagotribune.com/news/nationworld/ct-thailand-hot-april-20160427-story.html

Auffhammer, M., Baylis, P., & Hausman, C. H. (2017). Climate change is projected to have severe impacts on the frequency and intensity of peak electricity demand across the United States. *Proceedings of the National Academy of Sciences*, *114*(8), 1886–1891. https://doi.org/10.1073/pnas.1613193114

Beniston, M. (2004). The 2003 heat wave in Europe: A shape of things to come? An analysis based on Swiss climatological data and model simulations. *Geophysical Research Letters*, *31*(2), L02202. https://doi.org/10.1029/2003GL018857

Caesar, J., Alexander, L. V., Trewin, B., Tse-ring, K., Sorany, L., Vuniyayawa, V., et al. (2011). Changes in temperature and precipitation extremes over the Indo-Pacific region from 1971 to 2005. *International Journal of Climatology*, *31*(6), 791–801. https://doi.org/10.1002/joc.2118

Chang, C.-P., Wang, Z., McBride, J., & Liu, C.-H. (2005). Annual cycle of Southeast Asia—maritime continent rainfall and the asymmetric monsoon transition. *Journal of Climate*, *18*(2), 287–301. https://doi.org/10.1175/JCLI-3257.1

Coffel, E. D., Horton, R. M., & de Sherbinin, A. (2017). Temperature and humidity based projections of a rapid rise in global heat stress exposure during the 21st century. *Environmental Research Letters*, *13*(1), 014001. https://doi.org/10.1088/1748-9326/aaa00e

Cowan, T., Purich, A., Perkins, S., Pezza, A., Boschat, G., & Sadler, K. (2014). More frequent, longer, and hotter heat waves for Australia in the twenty-first century. *Journal of Climate*, *27*(15), 5851–5871. https://doi.org/10.1175/JCLI-D-14-00092.1

Dang, T. N., Honda, Y., Do, D. V., Pham, A. L. T., Chu, C., Huang, C. R., & Phung, D. (2019). Effects of extreme temperatures on mortality and hospitalization in Ho Chi Minh City, Vietnam. *International Journal of Environmental Research and Public Health*, *16*(3), 432. https://doi.org/10.3390/ijerph16030432

Dosio, A. (2017). Projection of temperature and heatwaves for Africa with an ensemble of CORDEX Regional Climate Models. *Climate Dynamics*, *49*(1–2), 493–519. https://doi.org/10.1007/s00382-016-3355-5

Dosio, A., Mentaschi, L., Fischer, E. M., & Wyser, K. (2018). Extreme heat waves under 1.5 °C and 2 °C global warming. *Environmental Research Letters*, *13*(5), 054006. https://doi.org/10.1088/1748-9326/aab827

Dunne, J. P., Stouffer, R. J., & John, J. G. (2013). Reductions in labor capacity from heat stress under climate warming. *Nature Climate Change*, *3*(6), 563–566. https://doi.org/10.1038/nclimate1827

Feng, J., Wang, L., Chen, W., Fong, S. K., & Leong, K. C. (2010). Different impacts of two types of Pacific Ocean warming on Southeast Asian rainfall during boreal winter. *Journal of Geophysical Research: Atmospheres*, *115*, D24122. https://doi.org/10.1029/2010jd014761

Fischer, E. M., & Schär, C. (2010). Consistent geographical patterns of changes in high-impact European heatwaves. *Nature Geoscience*, *3*(6), 398–403. https://doi.org/10.1038/ngeo866

Flato, G., Marotzke, J., Abiodun, B., Braconnot, P., Chou, S. C., Collins, W., et al. (2013). Evaluation of climate models. In T. F. Stocker, D. Qin, G. K. Plattner, M. Tignor, S. K. Allen, J. Boschung, et al. (Eds.), *Climate change 2013: The physical science basis. Contribution of working group I to the Fifth assessment Report of the intergovernmental Panel on climate change* (pp. 741–866). Cambridge University Press.

Grumm, R. H. (2011). The central European and Russian heat event of July–August 2010. *Bulletin of the American Meteorological Society*, *92*(10), 1285–1296. https://doi.org/10.1175/2011BAMS3174.1

Hamada, J. I., Yamanaka, M. D., Matsumoto, J., Fukao, S., Winarso, P. A., & Sribimawati, T. (2002). Spatial and temporal variations of the rainy season over Indonesia and their link to ENSO. *Journal of the Meteorological Society of Japan*, *80*(2), 285–310. https://doi.org/10.2151/jmsj.80.285

Huang, C., Cheng, J., Phung, D., Tawatsupa, B., Hu, W., & Xu, Z. (2018). Mortality burden attributable to heatwaves in Thailand: A systematic assessment incorporating evidence-based lag structure. *Environment International*, *121*, 41–50. https://doi.org/10.1016/j.envint.2018.08.058

Jenkinson, A. F. (1977). The analysis of meteorological and other geophysical extremes. *Synoptic Climatology Branch Memo*. the U.K. Met. Office. (Vol. *58*, p. 41).

Juneng, L., & Tangang, F. T. (2005). Evolution of ENSO-related rainfall anomalies in Southeast Asia region and its relationship with atmosphere–ocean variations in Indo-Pacific sector. *Climate Dynamics*, *25*(4), 337–350. https://doi.org/10.1007/s00382-005-0031-6

Kay, J. E., Deser, C., Phillips, A., Mai, A., Hannay, C., Strand, G., et al. (2015). The Community Earth System Model (CESM) large ensemble project: A community resource for studying climate change in the presence of internal climate variability. *Bulletin of the American Meteorological Society*, *96*(8), 1333–1349. https://doi.org/10.1175/BAMS-D-13-00255.1

Kjellstrom, T., Kovats, R. S., Lloyd, S. J., Holt, T., & Tol, R. S. J. (2009). The direct impact of climate change on regional labor productivity. *Archives of Environmental & Occupational Health*, *64*(4), 217–227. https://doi.org/10.1080/19338240903352776

Kravchenko, J., Abernethy, A. P., Fawzy, M., & Lyerly, H. K. (2013). Minimization of heatwave morbidity and mortality. *American Journal of Preventive Medicine*, *44*(3), 274–282. https://doi.org/10.1016/j.amepre.2012.11.015

Lesk, C., Coffel, E., D'Amato, A. W., Dodds, K., & Horton, R. (2017). Threats to North American forests from southern pine beetle with warming winters. *Nature Climate Change*, *7*(10), 713–717. https://doi.org/10.1038/nclimate3375

Li, D., Yuan, J., & Kopp, R. (2020). Escalating global exposure to compound heat-humidity extremes with warming. *Environmental Research Letters*, *15*, 064003. https://doi.org/10.1088/1748-9326/ab7d04

Li, X.-X. (2018). Linking residential electricity consumption and outdoor climate in a tropical city. *Energy*, *157*, 734–743. https://doi.org/10.1016/j.energy.2018.05.192

Li, X.-X. (2020). Heat wave trends in Southeast Asia during 1979–2018: The impact of humidity. *The Science of the Total Environment*, *721*, 137664. https://doi.org/10.1016/j.scitotenv.2020.137664

Lin, L. J., Chen, C. C., & Luo, M. (2018). Impacts of El Niño-Southern Oscillation on heat waves in the Indochina peninsula. *Atmospheric Science Letters*, *19*, e856. https://doi.org/10.1002/asl.856

Luo, M., & Lau, N.-C. (2018). Synoptic characteristics, atmospheric controls, and long-term changes of heat waves over the Indochina Peninsula. *Climate Dynamics*, *51*(7), 2707–2723. https://doi.org/10.1007/s00382-017-4038-6

Mann, H. B. (1945). Nonparametric tests against trend. *Econometrica*, *13*(3), 245–259. https://doi.org/10.2307/1907187. http://www.jstor.org/stable/1907187

Matthews, T. K. R., Wilby, R. L., & Murphy, C. (2017). Communicating the deadly consequences of global warming for human heat stress. *Proceedings of the National Academy of Sciences*, *114*(15), 3861–3866. https://doi.org/10.1073/pnas.1617526114

McBride, J. L., Haylock, M. R., & Nicholls, N. (2003). Relationships between the maritime continent Heat source and the El Niño–Southern oscillation phenomenon. *Journal of Climate*, *16*(17), 2905–2914. https://doi.org/10.1175/1520-0442(2003)016<2905:rbtmch>2.0.co;2

Meehl, G. A., & Tebaldi, C. (2004). More intense, more frequent, and longer lasting heat waves in the 21st century. *Science*, *305*(5686), 994–997. https://doi.org/10.1126/science.1098704

Mora, C., Dousset, B., Caldwell, I. R., Powell, F. E., Geronimo, R. C., Bielecki, C. R., et al. (2017). Global risk of deadly heat. *Nature Climate Change*, *7*(7), 501–506. https://doi.org/10.1038/nclimate3322

Morice, C. P., Kennedy, J. J., Rayner, N. A., & Jones, P. D. (2012). Quantifying uncertainties in global and regional temperature change using an ensemble of observational estimates: The HadCRUT4 data set. *Journal of Geophysical Research*, *117*, D08101. https://doi.org/10.1029/2011JD017187

National Academies of Sciences, Engineering, and Medicine. (2016). *Attribution of extreme weather events in the context of climate change*. The National Academies Press. https://doi.org/10.17226/21852

Perkins, S. E., & Alexander, L. V. (2013). On the measurement of heat waves. *Journal of Climate*, *26*(13), 4500–4517. https://doi.org/10.1175/JCLI-D-12-00383.1

Perkins, S. E., Alexander, L. V., & Nairn, J. R. (2012). Increasing frequency, intensity and duration of observed global heatwaves and warm spells. *Geophysical Research Letters*, *39*, L20714. https://doi.org/10.1029/2012gl053361

Perkins-Kirkpatrick, S. E., & Gibson, P. B. (2017). Changes in regional heatwave characteristics as a function of increasing global temperature. *Scientific Reports*, *7*(1), 12256. https://doi.org/10.1038/s41598-017-12520-2

Perkins-Kirkpatrick, S. E., & Lewis, S. C. (2020). Increasing trends in regional heatwaves. *Nature Communications*, *11*(1), 3357. https://doi.org/10.1038/s41467-020-16970-7

Pfahl, S., & Wernli, H. (2012). Quantifying the relevance of atmospheric blocking for co-located temperature extremes in the Northern Hemisphere on (sub-) daily time scales. *Geophysical Research Letters*, *39*, L12807. https://doi.org/10.1029/2012gl052261

Raymond, C., Matthews, T., & Horton, R. M. (2020). The emergence of heat and humidity too severe for human tolerance. *Science Advances*, *6*(19), eaaw1838. https://doi.org/10.1126/sciadv.aaw1838

Robertson, A. W., Moron, V., Qian, J.-H., Chang, C.-P., Tangang, F., Aldrian, E., et al. (2011). The maritime continent monsoon. In *The global monsoon system* (pp. 85–98). https://doi.org/10.1142/9789814343411_0006

Robine, J.-M., Cheung, S. L. K., Le Roy, S., Van Oyen, H., Griffiths, C., Michel, J.-P., & Herrmann, F. R. (2008). Death toll exceeded 70,000 in Europe during the summer of 2003. *Comptes Rendus Biologies*, *331*(2), 171–178. https://doi.org/10.1016/j.crvi.2007.12.001

Robinson, P. J. (2001). On the definition of a heat wave. *Journal of Applied Meteorology*, *40*(4), 762–775. https://doi.org/10.1175/1520-0450(2001)040<0762:otdoah>2.0.co;2

Russo, S., Sillmann, J., & Fischer, E. M. (2015). Top ten European heatwaves since 1950 and their occurrence in the coming decades. *Environmental Research Letters*, *10*(12), 124003. https://doi.org/10.1088/1748-9326/10/12/124003

Russo, S., Sillmann, J., & Sterl, A. (2017). Humid heat waves at different warming levels. *Scientific Reports*, *7*(1), 7477. https://doi.org/10.1038/s41598-017-07536-7

Schär, C. (2016). The worst heat waves to come. *Nature Climate Change*, *6*(2), 128–129. https://doi.org/10.1038/nclimate2864

Schoof, J. T., Ford, T. W., & Pryor, S. C. (2017). Recent changes in U.S. regional heat wave characteristics in observations and reanalyzes. *Journal of Applied Meteorology and Climatology*, *56*(9), 2621–2636. https://doi.org/10.1175/JAMC-D-16-0393.1

Sen, P. K. (1968). Estimates of the regression coefficient based on Kendall's Tau. *Journal of the American Statistical Association*, *63*(324), 1379–1389. https://doi.org/10.1080/01621459.1968.10480934

Seneviratne, S. I., Donat, M. G., Pitman, A. J., Knutti, R., & Wilby, R. L. (2016). Allowable CO2 emissions based on regional and impact-related climate targets. *Nature*, *529*(7587), 477–483. https://doi.org/10.1038/nature16542

Seneviratne, S. I., Nicholls, N., Easterling, D., Goodess, C. M., Kanae, S., Kossin, J., et al. (2012). *Changes in climate extremes and their impacts on the natural physical environment*. Cambridge Univ Press.

Stocker, T. F., Qin, D., Plattner, G. K., Tignor, M., Allen, S. K., Boschung, J., et al. (Eds.), (2013). *Climate change 2013: The physical science basis. Contribution of working group I to the Fifth assessment Report of the intergovernmental Panel on climate change*. Cambridge University Press.

Sun, X., Sun, Q., Zhou, X., Li, X., Yang, M., Yu, A., & Geng, F. (2014). Heat wave impact on mortality in Pudong New Area, China in 2013. *The Science of the Total Environment*, *493*, 789–794. https://doi.org/10.1016/j.scitotenv.2014.06.042

Sun, Y., Hu, T., & Zhang, X. (2018). Substantial increase in heat wave risks in China in a future warmer world. *Earth's Future*, *6*(11), 1528–1538. https://doi.org/10.1029/2018ef000963

Supari, Tangang, F., Juneng, L., & Aldrian, E. (2017). Observed changes in extreme temperature and precipitation over Indonesia. *International Journal of Climatology*, *37*(4), 1979–1997. https://doi.org/10.1002/joc.4829

Tebaldi, C., & Lobell, D. (2018). Estimated impacts of emission reductions on wheat and maize crops. *Climatic Change*, *146*(3), 533–545. https://doi.org/10.1007/s10584-015-1537-5

Thai Meteorological Department. (2017). Annual Weather Summary over Thailand in 2016. Available at https://www.tmd.go.th/en/climate.php?FileID=5

Thirumalai, K., DiNezio, P. N., Okumura, Y., & Deser, C. (2017). Extreme temperatures in Southeast Asia caused by El Niño and worsened by global warming. *Nature Communications*, *8*(1), 15531. https://doi.org/10.1038/ncomms15531

van den Besselaar, E. J. M., van der Schrier, G., Cornes, R. C., Iqbal, A. S., & Klein Tank, A. M. G. (2017). SA-OBS: A daily gridded surface temperature and precipitation dataset for Southeast Asia. *Journal of Climate*, *30*(14), 5151–5165. https://doi.org/10.1175/JCLI-D-16-0575.1

World Meteorological Organization. (2017). WMO statement on the state of the global climate in 2016. WMO-No., 1189, 1–28.

Xia, Y., Li, Y., Guan, D., Tinoco, D. M., Xia, J., Yan, Z., et al. (2018). Assessment of the economic impacts of heat waves: A case study of Nanjing, China. *Journal of Cleaner Production*, *171*, 811–819. https://doi.org/10.1016/j.jclepro.2017.10.069

Xu, P., Wang, L., Huang, P., & Chen, W. (2021). Disentangling dynamical and thermodynamical contributions to the record-breaking heatwave over Central Europe in June 2019. *Atmospheric Research*, *252*, 105446. https://doi.org/10.1016/j.atmosres.2020.105446

Xu, P., Wang, L., Liu, Y., Chen, W., & Huang, P. (2020). The record-breaking heat wave of June 2019 in Central Europe. *Atmospheric Science Letters*, *21*, 1–7. https://doi.org/10.1002/asl.964

You, Q., Jiang, Z., Kong, L., Wu, Z., Bao, Y., Kang, S., & Pepin, N. (2017). A comparison of heat wave climatologies and trends in China based on multiple definitions. *Climate Dynamics*, *48*(11), 3975–3989. https://doi.org/10.1007/s00382-016-3315-0

Zampieri, M., Ceglar, A., Dentener, F., & Toreti, A. (2017). Wheat yield loss attributable to heat waves, drought and water excess at the global, national and subnational scales. *Environmental Research Letters*, *12*(6), 064008. https://doi.org/10.1088/1748-9326/aa723b

Zhu, S. P., Ge, F., Fan, Y., Zhang, L., Sielmann, F., Fraedrich, K., & Zhi, X. F. (2020). Conspicuous temperature extremes over Southeast Asia: Seasonal variations under 1.5 °C and 2 °C global warming. *Climatic Change*, *160*(3), 343–360. https://doi.org/10.1007/s10584-019-02640-1